

Self-Assembly of Double-Stranded DNA Molecules at Nanomolar Concentrations[†]Shotaro Inoue,[‡] Shigeru Sugiyama,[§] Andrew A. Travers,^{||} and Takashi Ohyama^{*,1}

Department of Biology, Faculty of Science and Engineering, Konan University, 8-9-1 Okamoto, Higashinada-ku, Kobe 658-8501, Japan, Instrumentation Engineering Laboratory, National Food Research Institute, 2-1-12 Kannondai, Tsukuba, Ibaraki 305-8642, Japan, MRC Laboratory of Molecular Biology, Hills Road, Cambridge CB2 2QH, U.K., Department of Biology, Faculty of Education and Integrated Arts and Sciences, Waseda University, 1-6-1 Nishi-Waseda, Shinjuku-ku, Tokyo 169-8050, Japan, and Major in Integrative Bioscience and Biomedical Engineering, Graduate School of Science and Engineering, Waseda University, 1-6-1 Nishi-Waseda, Shinjuku-ku, Tokyo 169-8050, Japan

Received July 31, 2006; Revised Manuscript Received November 8, 2006

ABSTRACT: Some proteins have the property of self-assembly, known to be an important mechanism in constructing supramolecular architectures for cellular functions. However, as yet, the ability of double-stranded (ds) DNA molecules to self-assemble has not been established. Here we report that dsDNA molecules also have a property of self-assembly in aqueous solutions containing physiological concentrations of Mg²⁺. We show that DNA molecules preferentially interact with molecules with an identical sequence and length even in a solution composed of heterogeneous DNA species. Curved DNA and DNA with an unusual conformation and property also exhibit this phenomenon, indicating that it is not specific to usual B-form DNA. Atomic force microscopy (AFM) directly reveals the assembled DNA molecules formed at concentrations of 10 nM but rarely at 1 nM. The self-assembly is concentration-dependent. We suggest that the attractive force causing DNA self-assembly may function in biological processes such as folding of repetitive DNA, recombination between homologous sequences, and synapsis in meiosis.

Protein molecules make assemblies by intermolecular interactions, and various molecular machines and subcellular structures are formed by these assemblies. When a molecule or a few kinds of molecules assemble, “protein polymers” which have regular structures are formed. Tobacco mosaic virus (TMV)¹ is an early example of such a phenomenon. TMV is decomposed into an RNA and proteins at acidic pH, and the virus is reformed by forming a protein polymer on the RNA with rising pH (1). In this case, polymerization occurs toward the state of minimum free energy, which is determined by such conditions including the chemical potentials of molecules and ions, temperature, and pH (2). This kind of protein polymerization has been called “self-assembly” (2, 3). Actin, myosin, and tubulin in eukaryotic cells and flagellin found in bacterial flagella are also well-known examples of the molecules that exhibit a self-assembly phenomenon (4–7).

Two single-stranded DNA or RNA strands with complementary nucleotide sequences form double-stranded helices, which may be considered to be the simplest form of the assembly of nucleic acids. It is also known that nine GGA sequence repeats form a parallel-stranded DNA homoduplex

in the presence of 50 mM NaCl at pH 4, 7, and 9 (8). Furthermore, DNA and RNA molecules can also assemble to form multistranded structures such as triplex and quadruplex structures in a nucleotide sequence-dependent manner, through base pairing [e.g., Watson–Crick, Hoogsteen, and reverse Hoogsteen (9, 10)]. In very concentrated solutions, even dsDNA molecules assemble regularly, which finally results in generation of DNA crystals (11). However, the ability of dsDNA molecules to assemble at nanomolar concentrations has not been demonstrated.

We have previously reported that electrophoresis using physiological concentrations of Mg²⁺ can cause a mobility shift of restriction fragments in nondenaturing polyacrylamide gels as the overhangs interact (12). Theoretically, this phenomenon can be used to detect preferential intermolecular DNA interactions, if any, in aqueous solutions. Using a facile method, we studied the intermolecular DNA interactions and found that DNA molecules with an identical sequence and length preferentially interact with each other and self-assemble even in a solution composed of heterogeneous DNA species. In this report, we show for the first time that dsDNA molecules have the property of self-assembly.

MATERIALS AND METHODS

DNA Preparation. Fragments A and AR, B and BR, and C and CR originated from *Hind*III–*Hinc*II, *Hind*III–*Bam*HI, and *Hind*III–*Eco*RV fragments of pBR322, respectively. The *Hind*III site of the plasmid was converted to a *Mlu*I site in constructs A, B, and C. In the construction of fragments AR, BR, and CR, the *Hinc*II, *Bam*HI, and *Eco*RV sites, respectively, were converted to *Mlu*I sites. Fragment D originated from the *Eco*RV–*Eco*T14I fragment of pGL2-Basic Vector

[†] This study was supported in part by JSPS and MEXT research grants to T.O.

* To whom correspondence should be addressed. E-mail: ohyama@waseda.jp. Telephone: +81 3 5286 1520. Fax: +81 3 3207 9694.

[‡] Konan University.














[§] National Food Research Institute.

^{||} MRC Laboratory of Molecular Biology.

¹ Faculty of Education and Integrated Arts and Sciences and Graduate School of Science and Engineering, Waseda University.

¹ Abbreviations: ds, double-stranded; AFM, atomic force microscopy; TMV, tobacco mosaic virus.

Table 1: DNA Fragments Used in This Study

Name (length ^a)		Structure ^b	Type
A	(631 bp)	CGCGTC AG 	B-form
B	(357 bp)	CGCGTC AG 	B-form
C	(165 bp)	CGCGTC AG 	B-form
AR	(631 bp)	 GA CTGCGC	B-form
BR	(359 bp)	 GA CTGCGC	B-form
CR	(165 bp)	 GA CTGCGC	B-form
D	(789 bp)	CGCGTC AG 	B-form
DRA	(615 bp)	 GA CTGCGC	B-form
DB	(351 bp)	CGCGTC AG 	B-form
EL	(743 bp)		B-form / blunt
ES	(277 bp)		B-form / blunt
F	(257 bp)	CGCGTC AG 	bent
G	(118 bp)	CGCGTC AG 	A-form-like ^c

^a Only the double-stranded portion is counted. ^b To indicate the sameness or difference in the sequence of DNA fragments, colored bars are used. ^c The fragment exhibits anomalously fast migration in nondenaturing polyacrylamide gels. The partial formation of an A-form-like structure and its rigid nature seem to be the cause of the phenomenon (15, 18).

(Promega), and the *EcoRV* site was converted to a *MluI* site. The plasmids with a newly created *MluI* site were cleaved at the non-*MluI* sites indicated above, treated with T4 DNA polymerase (except in the case of *HincII* cleavage), and finally digested with *MluI*. The resulting fragments were cloned between the *MluI* and *SmaI* sites of pUC19-MS with *MluI* and *HincII*–*SmaI*–*HincII* sites (instead of the *SmaI* and *HincII* sites, respectively). To prepare fragment F (carrying two bent DNAs), a *Bam*HI fragment containing the bent DNA of the human adenovirus type 2 *E1A* enhancer (13) was obtained from a construct with the *AccI*–*SacII* region of the enhancer at the *SmaI* site of pPRT-5/4 (12). Using blunt end ligation, the fragment was inserted into the *KpnI* site of pLHC4/TLN-6 (14), which contains a synthetic bent DNA. The resulting construct was cleaved with *AatII*, treated with T4 DNA polymerase, and digested with *MluI*. The *AatII* (blunt)–*MluI* fragment was cloned between the *MluI* and *SmaI* sites of pUC19-MS described above. Fragment G was derived from the *PstI*–*StuI* fragment within a 0.7 kb *PstI* fragment of bovine satellite I DNA (15) cloned into pUC19. After the *StuI* site was converted to a *MluI* site, the construct was cleaved with *HincII* and *MluI* and cloned into pUC19-MS. By digesting all of the insert-carrying pUC19-MS plasmids with *MluI* and *HincII*, we obtained the required fragments. Fragments EL and ES were obtained by digesting A-carrying pUC19-MS and C-carrying pUC19-MS with *HincII* and *PvuII*.

To generate fragment DRA, fragment DR (not listed in Table 1) was first prepared; i.e., the *EcoT14I* site of the pGL2 vector was converted to a *MluI* site, and this vector was

digested with *EcoRV* and *MluI* to produce fragment DR. After fragment DR was cloned into pUC19-MS, the resulting construct was digested with *BsrI*, treated with T4 DNA polymerase, and digested with *MluI*. Fragment DB was obtained by digesting fragment D with *AluI*.

Electrophoresis on DEAE-cellulose paper was used to recover the DNA fragments. After phenol extraction and ethanol precipitation, DNA fragments were dissolved in TBN buffer comprised of $\frac{1}{2} \times$ TB [45 mM Tris-borate (pH 8.3)] and 10 mM NaCl. To remove possible contaminants, each fragment solution was loaded onto a MicroSpin G-25 column (Amersham Biosciences) and centrifuged. The fragments were then precipitated with ethanol, rinsed, dried, and dissolved in TBN buffer.

Labeling of 5'-termini with [γ -³²P]ATP was performed using a standard protocol (16). The reaction mixture was extracted with phenol and passed through a MicroSpin G-25 column. The labeled fragments were precipitated with ethanol, rinsed twice, dried, and dissolved in TBN buffer at a concentration of 6 fmol/ μ L.

Electrophoresis. Unless otherwise indicated, electrophoresis was carried out as follows. A 10 μ L sample solution containing radiolabeled DNA fragments (600 pM each), one of the cold DNA fragments at 1–30 nM, and 1, 20, or 25 mM MgCl₂ was prepared in TBN buffer. Each sample was prepared in stages. First, 1 μ L solutions of each radiolabeled DNA were mixed; then, a 5 μ L solution containing cold DNA fragments in the same buffer was added to the mixture and mixed by pipetting, and finally, 2 μ L of 5, 100, or 125 mM MgCl₂ was added to the solution and mixed in the same

way. Samples without cold DNA were also prepared by adding TBN buffer instead of a cold DNA solution. The samples were then electrophoresed on 7.5% polyacrylamide (29:1 acrylamide:bisacrylamide ratio) gels at 5 or 10 °C. The gels contained a running buffer of $\frac{1}{2} \times$ TB with 1, 20, or 25 mM MgCl_2 . The electrophoretic field across the gels was maintained at 10.8 V/cm. The buffer solution was pumped between the electrode compartments as described previously (12).

DNA Ligation. Solutions were prepared containing 7 fmol of each of the 5'-end-labeled fragments, A and C (solution I, 1.5 μL), 24 fmol of cold A or C (solution II, 8.5 μL), 12 mM MgCl_2 (solution III, 2 μL), and 10 units of T4 DNA ligase, 257 mM Tris-HCl (pH 8.0), 33 mM KCl, 6 mM DTT, 5 mM ATP, and 33% glycerol (solution IV, 3 μL). Solutions I–III were placed separately on the inside wall of a 1.5 mL Eppendorf tube, collected when the tubes were spun down, and mixed by tapping. One or ten minutes after the spin down, solution IV was added and mixed by pipetting. Ligation was performed at 10 °C for 15 min. In the procedure without preincubation, the four solutions were mixed at the same time and incubated. Reactions were stopped by extraction with phenol, and after purification, the samples were electrophoresed on 1% agarose gels. Solution I and a mixture of solutions I and II were electrophoresed as unligated controls. DNA bands were detected by autoradiography.

AFM Observations. Topographic images of DNA were observed with an NVB100 atomic force microscope (Olympus Optical Co. Ltd.) fitted with a NanoScope IIIa controller (Digital Instruments). The atomic force microscope was operated in tapping mode in air at room temperature. A silicon cantilever (Olympus Optical Co. Ltd., OMCL-AC160TS-C2) with an oscillation frequency of 300 kHz and a spring constant of 42 N/m was used. As the substrate for the AFM observation, 3-aminopropyltriethoxysilane (APTES)-coated mica was used. APTES coating was performed by the vapor method under a nitrogen atmosphere at room temperature as described by Sasou et al. (17). An aliquot of DNA (20 or 2 fmol/ μL) in TBN was mixed with an equal volume of TBN supplemented with 5 mM MgCl_2 and incubated for 10 min at room temperature. Then 1 μL of the solution was dropped onto the substrate surface, and after a 10 s incubation period, the solution was rapidly soaked up and the surface air-dried.

RESULTS

DNA Molecules Self-Assemble in Aqueous Solutions. To electrophoretically detect intermolecular interaction of DNA fragments, we first prepared DNA fragments with one blunt end and the other end with a 5'-overhang of the 5'-CGCG sequence (Table 1) and used the procedure illustrated in Figure 1A. Fragments B and C were derived from fragment A. Thus, they share a common sequence. Fragments AR, BR, and CR attach the 5'-CGCG overhang at the other end of fragments A, B, and C, respectively. This is the only difference between the two groups. Radiolabeled fragments A, B, and C (A^* , B^* , and C^* , respectively; 600 pM each) electrophoresed normally when cold DNA was absent (lanes with a minus sign in Figure 1B–D). However, when the concentration of one of the fragments was increased with

unlabeled fragments before addition of MgCl_2 , reduced mobility and smearing of the corresponding bands occurred in a concentration-dependent manner (Figure 1B, top three panels). The final concentrations of fragments in each tube were as follows: lanes 2, 6, and 10, each radioactive DNA fragment at 600 pM and 1 nM cold DNA; lanes 3, 7, and 11, each radioactive DNA fragment at 600 pM and 6 nM cold DNA; and lanes 4, 8, and 12, each radioactive DNA fragment at 600 pM and 30 nM cold DNA. As a test to determine the effect of a higher concentration of cold DNA fragments, we also incubated 60 or 120 nM cold A in the mixture of A^* , B^* , and C^* . However, the band-shift patterns were the same as that of lane 4 (not shown). The effects on the band-shift pattern of AR, BR, and CR were only slightly weaker than those of A, B, and C, respectively (Figure 1B, bottom three panels), which is scrutinized later.

Fragments DRA and DB differ from A and B, respectively, in sequence but are similar in length. Although DRA selectively interacted with A^* (Figure 1C), the effect of the DRA was weaker than those of A and AR (Figure 1B). Similarly, the interaction between DB and B^* was slightly weaker than the interaction between B and B^* and that between BR and B^* (Figure 1B,C). These slight differences are clear in Figure 1D. Since the effect of sequence homology on the intermolecular interaction became clear in these experiments using fragments DRA and DB, we did not prepare a DNA fragment of ~ 165 bp in B-form lacking any homology with fragment C, and we did not include a control experiment using such a fragment. In conclusion, the strongest interaction was found between identical molecules (hot vs cold fragments). The second strongest was the interaction between molecules and the “quasi-identical” molecules. We also studied the intermolecular interaction among “usual” B-DNA (fragment D), bent DNA (fragment F), and DNA with an unusual conformation and property [fragment G (15, 18)]. As shown in Figure 1E, both fragments F and G selectively interacted with their cold counterparts as well. Therefore, self-interactions are not confined within usual B-form DNAs. The phenomenon reported here was Mg^{2+} ion-dependent and was not observed in the absence of MgCl_2 (Figure 1F), which clearly excludes the possibility that an increased amount of DNA in a lane might have caused the retarded migration of DNA molecules. All of the electrophoreses described above were performed at 10 °C. To determine the effect of temperature on the phenomenon, we also examined the interaction among fragments A^* , B^* , C^* , and A at 20 °C. Although the extents were reduced, the retarded migration of A^* was clearly observed in 6 and 30 nM cold A lanes (not shown).

Figure 1 clearly indicates the presence of some mechanism that distinguishes self from nonself. Then, how did the retarded migration of DNA molecules occur? This phenomenon can be explained in terms of DNA self-assembly. The assembled molecules would migrate more slowly than the nonassembled constituents. In an experiment using DNA fragments with two cohesive ends, we previously observed more pronounced band shifts or smearing (12), while in the study, we did not observe retarded migration of the fragments with blunt ends. On the basis of these observations, we argued that cohesive ends form stable base pairings that resist electrophoretic separation. The critical difference between the previous study and this one is the number of species of

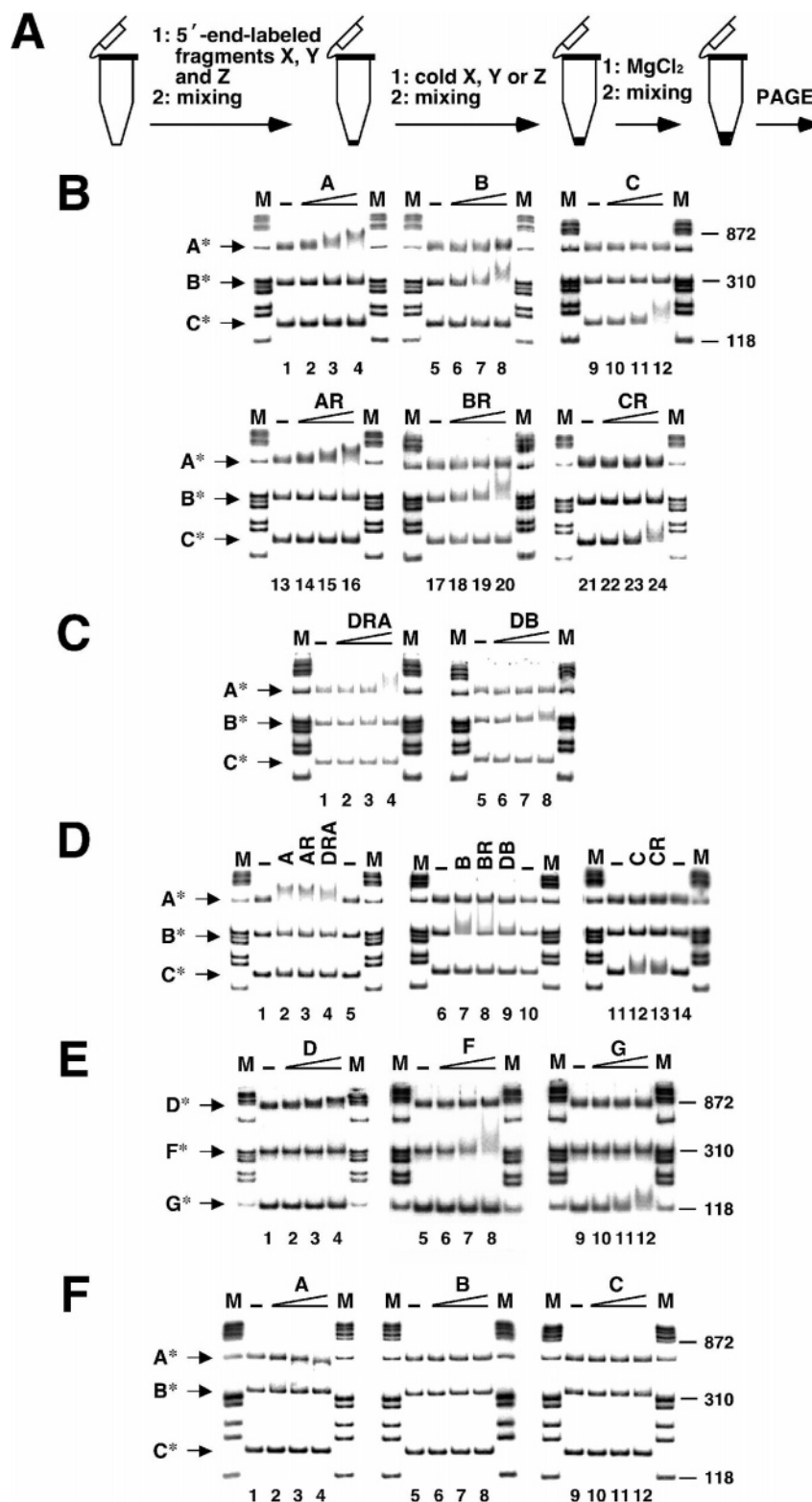


FIGURE 1: Selective interaction between dsDNA molecules as detected by electrophoresis. (A) Mixing procedure of DNA fragments. X, Y, and Z symbolize DNA fragments. Sample solutions each contained 1 mM MgCl₂, and electrophoreses were carried out at 10 °C. (B) Preferential interaction between identical or quasi-identical DNA molecules in the mixture of DNA fragments. The radiolabeled fragments (600 pM each) are denoted with an asterisk. Concentrations of added cold DNAs were as follows: lanes 1, 5, 9, 13, 17, and 21, no cold DNA added; lanes 2, 6, 10, 14, 18, and 22, 1 nM cold DNA added; lanes 3, 7, 11, 15, 19, and 23, 6 nM cold DNA added; and lanes 4, 8, 12, 16, 20, and 24, 30 nM cold DNA added. M lanes contained markers (mixture of *Hae*III digest of phage ϕ X174 DNA and the 1748 bp *Hinc*II–*Sca*I fragment of pUC19). (C) Interaction between nonidentical DNA molecules with approximately the same length: lanes 1 and 5, no cold DNA added; lanes 2 and 6, 1 nM cold DNA added; lanes 3 and 7, 6 nM cold DNA added; and lanes 4 and 8, 30 nM cold DNA added. (D) Demonstration of the superiority of the sameness in the selective interaction: lanes 1, 5, 6, 10, 11, and 14, no cold DNA added; and the other lanes, 10 nM cold DNA added. (E) Effect of DNA conformation and property on the interaction: lanes 1, 5, and 9, no cold DNA added; lanes 2, 6, and 10, 1 nM cold DNA added; lanes 3, 7, and 11, 6 nM cold DNA added; and lanes 4, 8, and 12, 30 nM cold DNA added. (F) A control experiment conducted in the absence of MgCl₂.

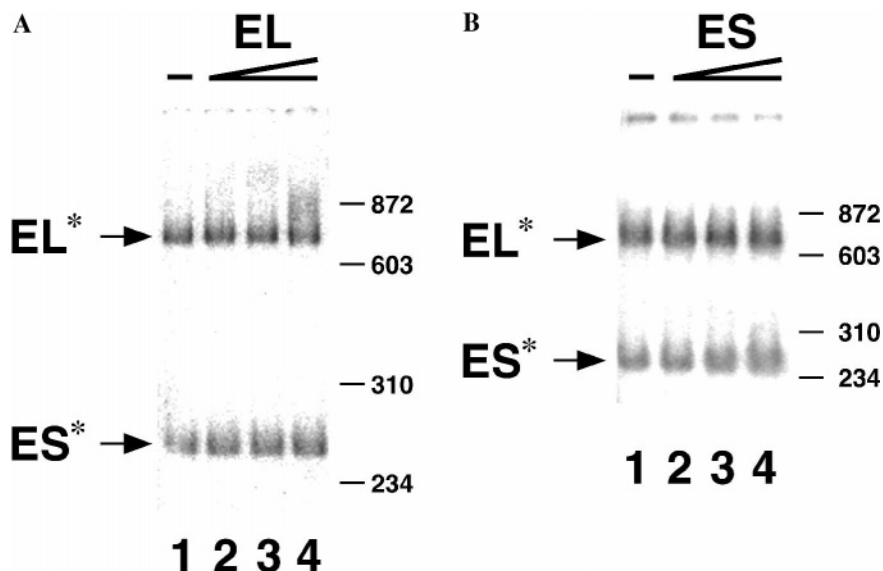


FIGURE 2: Electrophoretic detection of assembled DNA molecules with blunt ends. Cold fragment EL (743 bp) or ES (277 bp) was added to the mixture of radiolabeled fragments EL and ES (600 pM each) according to the procedure shown in Figure 1A. In panel A, the electrophoresis was carried out at 7.7 V/cm and 5 °C in the presence of 20 mM MgCl_2 . In panel B, using a 4% polyacrylamide gel, the electrophoresis was carried out at 5 °C in the presence of 25 mM MgCl_2 . The other conditions were the same as those used in Figure 1. In each panel, concentrations of the added cold fragment were as follows: lane 1, no cold DNA added; lane 2, 1 nM cold DNA added; lane 3, 6 nM cold DNA added; and lane 4, 30 nM cold DNA added.

DNA molecules in a sample solution; i.e., only a single species was contained in the samples in the previous study, while multiple species were contained in the samples in this study. We can reinterpret the phenomenon observed in the previous study as follows. DNA first self-assembled in the presence of MgCl_2 ; then, the assemblies were stabilized by end-to-end base pairings between constituent molecules.

To substantiate this hypothesis, we need to prove that DNA molecules can self-assemble irrespective of the form of fragment ends. Thus, we scrutinized the electrophoretic behavior of a mixture of blunt-ended DNA fragments. By increasing the concentration of surrounding Mg^{2+} ions, we could detect a selective (or preferred) interaction between the EL molecules in the mixture of fragments EL and ES (Figure 2A, lanes 3 and 4). When a rectangle, formed by the bandwidth of EL^* (the long side) and its half-length (the short side), was placed on the EL^* in lane 1, it contained most of the radioactivity of the fragment. Therefore, we quantified the smear in the upstream of this rectangle. The increases of the smear were 1.8-fold in lane 2, 1.3-fold in lane 3, and 6.4-fold in lane 4. We also analyzed lanes 1–4 in Figure 1B with the same method. The obtained values were 7.2-fold in lane 2, 23.8-fold in lane 3, and 41.2-fold in lane 4. Thus, the smear (band-shift rather than smear in Figure 1B) was quantified as being much greater in the case of the DNA fragments with a cohesive end. Using a gel with a lower polyacrylamide concentration (4%) and a further increasing MgCl_2 concentration (25 mM), a trace of the selective interaction between ES molecules was also narrowly detectable (Figure 2B, lane 4). Thus, the same phenomenon as that shown in Figure 1 could be shown by using the mixture of blunt-ended DNA fragments. However, the assemblies of blunt-ended DNA fragments and especially those of short DNA fragments seem to be fragile. The data from this experiment also suggest that the electrophoretic condition used in the previous study, in which shorter DNA fragments (~140–180 bp) were electrophoresed at a lower

concentration of MgCl_2 (1 or 10 mM) by using 7.5% polyacrylamide gels (12), was not suitable for the electrophoretic detection of assemblies of blunt-ended DNA molecules. Accordingly, we conclude that self-assembly of DNA molecules occurs in a Mg^{2+} -containing solution irrespective of the form of the fragment ends.

Kinetics of DNA Self-Assembly. The preparation and loading of multiple samples for electrophoresis normally take several minutes. To investigate the kinetics of self-recognition, we performed ligation reactions. A DNA concentration of 10 nM allowed interaction between nonidentical molecules A^* and DRA and also between B^* and DB (Figure 1D). In contrast, a concentration of 1 nM allowed, although only to a very limited extent, only the interaction between identical molecules (Figure 1B; broadening of bands A^* and B^* was observed in lanes 2 and 6, respectively). Thus, the ligation reaction was performed under conditions similar to this so preferential interactions could be detected. For this experiment, we used fragments A and C. As shown in Figure 3, the reactions were very inefficient (lanes 3–5 and 8–10). However, the results were largely consistent with those obtained in the electrophoretic experiments; i.e., although molecules A–C were generated in detectable amounts, greater amounts of both A–A and C–C molecules were also detected. Digestions of the ligation products with *MluI* or *HincII* showed that they were ligated at *MluI* ends (not shown). The electrophoretic assay thus appears to be more selective than the ligation assay. One possible reason for this is that the ligation assay traps the more transient interactions that would be too labile to be detected by electrophoresis.

AFM Images of the Assembled Molecules. The self-assembly of DNA fragments was confirmed by AFM. The representative images are shown in Figure 4. Initially, fragment A which has 631 bp (~210 nm) was used in the observation. Some thick DNA fibers with a height of >1 nm were observed when a 10 nM DNA solution was used (Figure 4A,D). Since the height of a single dsDNA observed

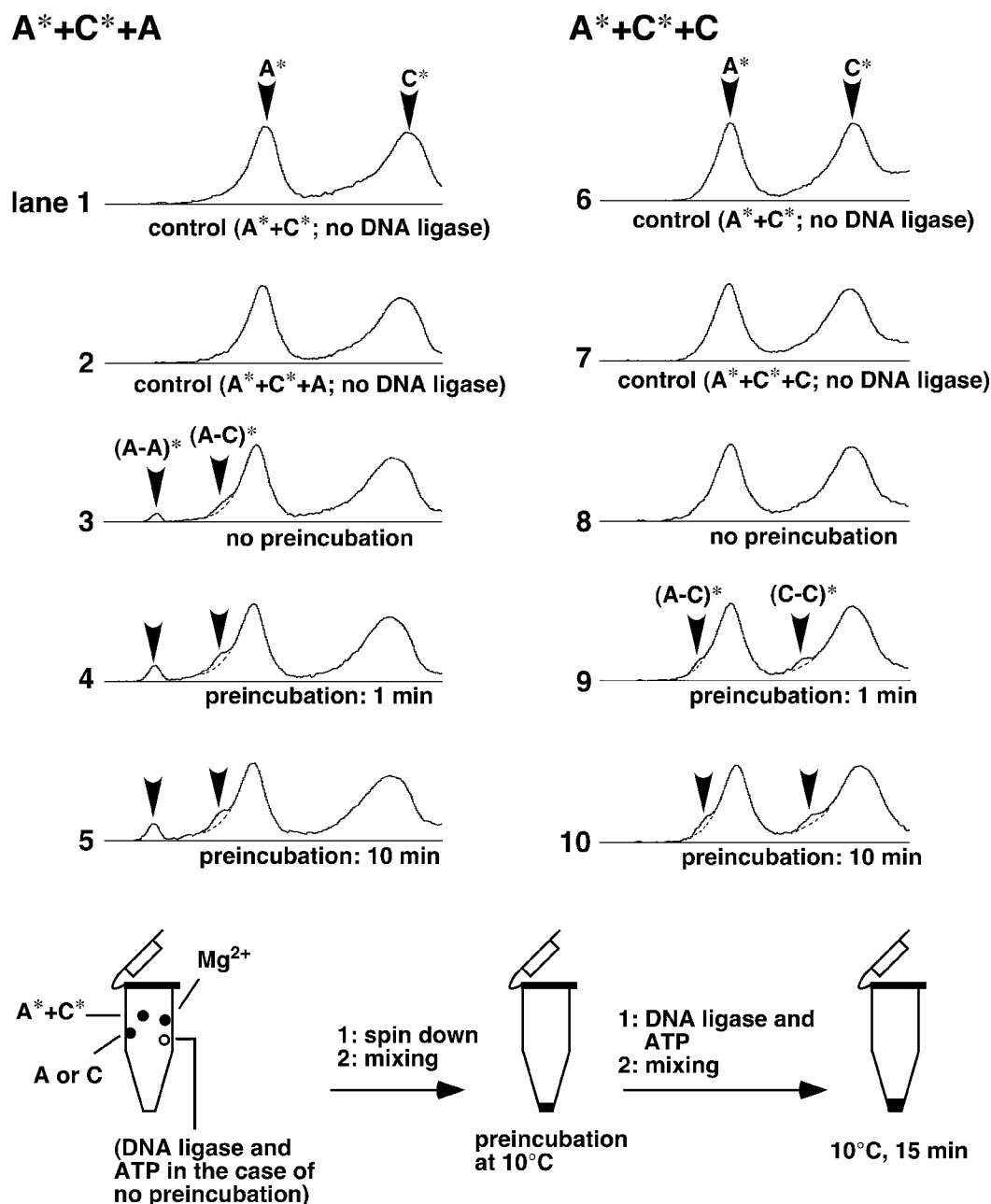


FIGURE 3: Time required for the selective interaction as measured by DNA ligation. Experimental conditions are summarized at the bottom. Ligation products were separated on 1% agarose gels, and densitometric analyses were performed. Shown are the results. A and C represent fragments A and C, respectively, and A* and C* represent 5'-end-labeled fragments A and C, respectively. The positions of fragments are denoted with arrowheads. (A-A)*, (C-C)*, and (A-C)* represent ligated molecules. The dashed lines in parts 3–5 were drawn on the basis of the line in part 2, and those in parts 9 and 10 were based on the line in part 7.

by AFM in air was reported to be less than 1 nm (17), these thick DNA fibers were possibly made of multiple (several) dsDNA molecules. Most of them have an approximate length of 200 nm, which is almost the same as the length of fragment A, indicating that very neat bunches of fragment A formed. Interestingly, a Y-shaped fiber, which indicates a decomposing (or forming) bunch, is observed near the center of the upper half in Figure 4A. Furthermore, in several bunches, one end is thicker than the other. The bulged ends may have been caused by the end-to-end base pairings, for such base pairings should require bowed ends of DNA molecules. We can also observe the thick and long fibers of an approximate length of 400 nm, which are considered to be dimers of the bunched dsDNAs. They were presumably formed through end-to-end base pairings between constituent

fragments in any two DNA bunches. Fragment EL of 743 bp (~250 nm) that has two blunt ends also formed thick fibers (Figure 4B,E), confirming that the DNA self-assembly is independent of the form of the fragment ends. In contrast, when a 1 nM DNA solution was subjected to AFM observation, as shown panels C and F of Figure 4, the heights of DNA fibers were usually less than 1 nm, indicating that each fiber was a single dsDNA.

Because of the narrow observation area, the observed DNA type (bunched or single) was sometimes “region specific”; for example, even on the mica of Figure 4A, some areas exclusively contained thick DNAs assumed to be the bunched forms, and some areas had only fine DNAs (single molecules). However, the ratio of thick DNAs to fine DNAs in the 10 fmol/ μ L solution was much higher than that

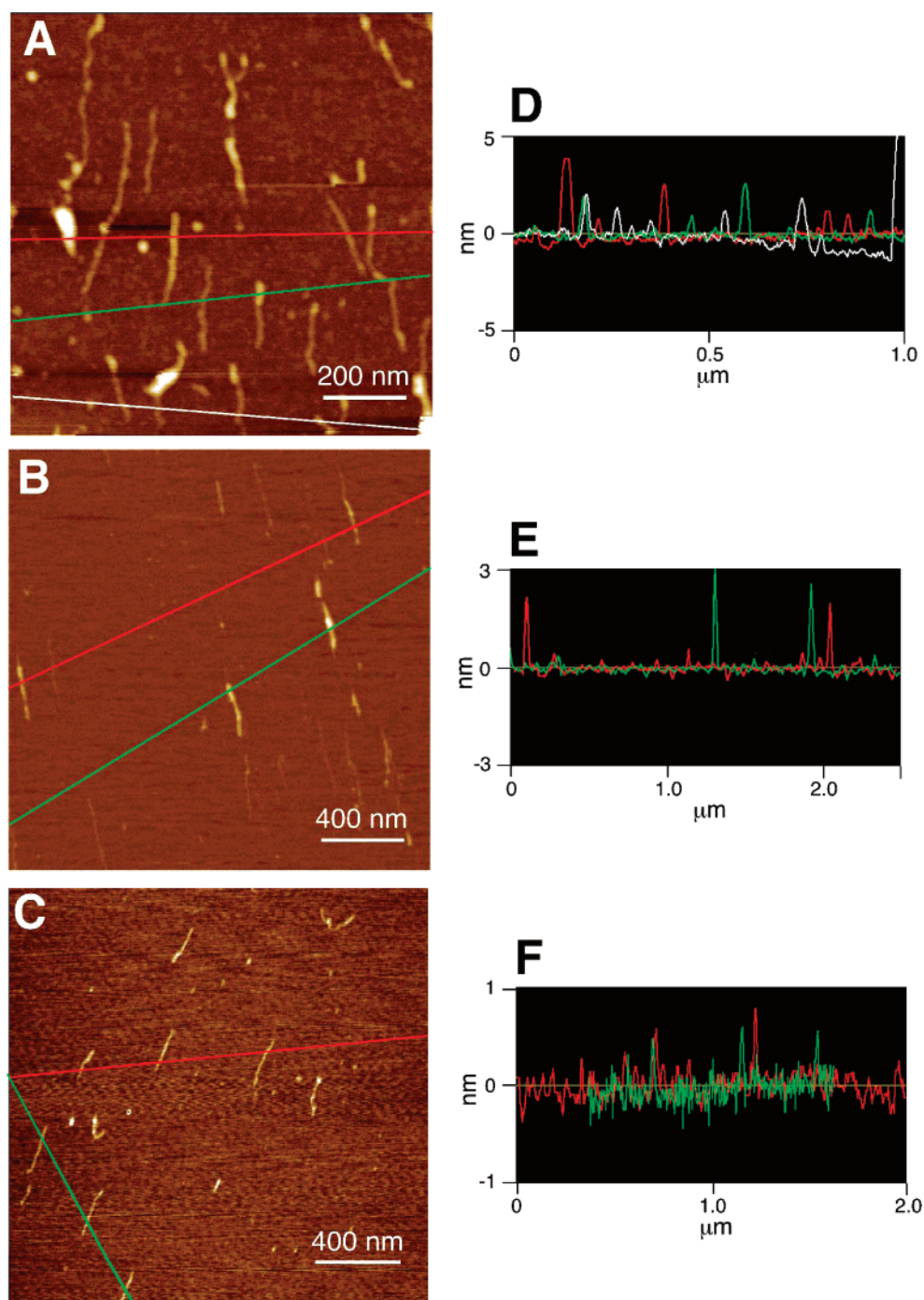


FIGURE 4: AFM observation of DNA at high and low concentrations. (A) Topographic image of fragment A at a high concentration (10 fmol/μL). The scan range was $1 \times 1 \mu\text{m}^2$. The height range was 5 nm. (B) Topographic image of fragment EL at a high concentration (10 fmol/μL). The scan range was $2 \times 2 \mu\text{m}^2$. The height range was 3 nm. (C) Topographic image of fragment A at a low concentration (1 fmol/μL). The scan range was $2 \times 2 \mu\text{m}^2$. The height range was 1 nm. (D) Section profiles along the colored lines (red, green, and white) in panel A. (E) Section profiles along the red and green lines in panel B. (F) Section profiles along the red and green lines in panel C.

in the 1 fmol/μL solution. Furthermore, the image in which almost all DNAs were bunched was only obtained when we used a 10 fmol/μL solution of fragment A (having a cohesive end). Thus, the microscopic fields shown in Figure 4 were chosen as the representative images under the respective conditions.

DISCUSSION

This study clearly demonstrates that the self-assembly of DNA molecules occurs at nanomolar concentrations in the

presence of physiological concentrations of MgCl_2 , irrespective of the form of fragment ends. The self-assemblies seem to be considerably stabilized when the molecules can base pair between the ends. The mechanism underlying the phenomenon in Figure 1 can be explained as follows; at first, the identical DNA molecules self-assemble with the aid of Mg^{2+} ions; second, end-to-end base pairings form between the fragments in each assembly, and finally, the base pairings stabilize DNA assemblies to such an extent that they resist decomposition caused by the electrophoretic friction. If the

self-assembly had not occurred, all combinations of base-paired DNA fragments should have been detected in Figure 1.

A Putative Mechanism of DNA Self-Assembly and Its Biological Relevance. What is the molecular basis of self-recognition? Our results indicate that this phenomenon most strongly favors identical lengths and sequences. Furthermore, this phenomenon needs magnesium ions, which is clearly shown in Figure 1. Magnesium ions normally alleviate electrostatic repulsive interactions between phosphates, thereby both stabilizing the sugar–phosphate backbone of DNA (19) and allowing the close approach of DNA duplexes. The favored sites for direct coordination to magnesium are the phosphate oxygen and N7 and O6 of guanosine (20, 21). This kind of coordination may be possible in intermolecular interactions. If intermolecular phosphate coordination were preferred over intramolecular coordination, the assembly of DNA molecules of equal length would be favored. Nevertheless, such a phenomenon would be insufficient to explain the dependence on DNA sequence. However, even in the presence of magnesium ions, the DNA duplex is labile on a millisecond time scale, allowing local bubble formation as well as base flipping (22). One possibility is that the magnesium-dependent alignment of DNA molecules of identical sequence and length could be stabilized by such perturbations occurring simultaneously (and transiently) at identical positions in the sequence. These transient perturbations would tend to be suppressed at higher magnesium concentrations, and under these conditions, the interactions would exhibit a lower specificity. Indeed, in the electrophoretic analysis at higher magnesium concentrations, we also detected a slight retardation of band B* in the presence of 30 nM cold fragment A (not shown), indicating that the molecules with different sizes began to assemble under the condition. Thus, the self-assembly of DNA without contamination of different DNA species seems to occur in a limited range of magnesium and DNA concentrations. Interestingly, the concentration required for DNA self-assembly is far below that for polymerization of flagellin (5).

Do the fragment ends play a role in interfragment interactions? As shown in Figures 2 and 4 (B and E), the end structure of DNA is irrelevant to the self-assembly per se. Furthermore, the following point strengthens this conclusion. If the end-to-end interaction between cohesive ends functioned to trigger the molecular assembly, we would have expected to observe nonbunched dimer molecules that were simply composed of two dsDNA molecules. However, we did not observe such molecules in the atomic force microscope.

Large structures may most efficiently be built by repetition of smaller ones. The attractive force working between the same sequences may be used in various biological processes, including DNA. For example, it may be used, in part, to construct centromeres and telomeres by folding repetitive DNA sequences. Furthermore, the force may be used in DNA recombination between homologous sequences and synapsis in meiosis.

ACKNOWLEDGMENT

We acknowledge the contributions of Mitsunori Morita and Junko Ohyama.

REFERENCES

1. Fraenkel-Conrat, H., and Williams, R. C. (1955) Reconstitution of active tobacco mosaic virus from its inactive protein and nucleic acid components, *Proc. Natl. Acad. Sci. U.S.A.* **41**, 690–698.
2. Oosawa, F., and Asakura, S. (1975) *Thermodynamics of the polymerization of protein*, Academic Press, London.
3. Kushner, D. J. (1969) Self-assembly of biological structures, *Bacteriol. Rev.* **33**, 302–345.
4. Horvath, I., Kiraly, C., and Szerb, J. (1949) Action of cardiac glycosides on the polymerization of actin, *Nature* **164**, 792.
5. Asakura, S. (1968) A kinetic study of *in vitro* polymerization of flagellin, *J. Mol. Biol.* **35**, 237–239.
6. Miki-Noumura, T., and Mori, H. (1972) Polymerization of tubulin: The linear polymer and its side-by-side aggregates, *J. Mechanochem. Cell Motil.* **1**, 175–188.
7. Miyahara, M., and Noda, H. (1977) Self-assembly of myosin *in vitro* caused by rapid dilution: Effects of hydrogen ion, potassium chloride, and protein concentrations, *J. Biochem.* **81**, 285–295.
8. Suda, T., Mishima, Y., Asakura, H., and Kominami, R. (1995) Formation of a parallel-stranded DNA homoduplex by d(GGA) repeat oligonucleotides, *Nucleic Acids Res.* **23**, 3771–3777.
9. Liu, H., Matsugami, A., Katahira, M., and Uesugi, S. (2002) A dimeric RNA quadruplex architecture comprised of two G:G(A):G:G(A) hexads, G:G:G:G tetrads and UUUU loops, *J. Mol. Biol.* **322**, 955–970.
10. Van Dyke, M. W. (2005) Do DNA triple helices or quadruplexes have a role in transcription?, in *DNA Conformation and Transcription* (Ohshima, T., Ed.) pp 105–126, Landes Bioscience, Georgetown, TX, and Springer, New York.
11. Timsit, Y., and Moras, D. (1992) Crystallization of DNA, *Methods Enzymol.* **211**, 409–429.
12. Tagashira, H., Morita, M., and Ohyama, T. (2002) Multimerization of restriction fragments by magnesium-mediated stable base pairing between overhangs: A cause of electrophoretic mobility shift, *Biochemistry* **41**, 12217–12223.
13. Ohyama, T. (1996) Bent DNA in the human adenovirus type 2 E1A enhancer is an architectural element for transcription stimulation, *J. Biol. Chem.* **271**, 27823–27828.
14. Nishikawa, J., Amano, M., Tanaka, S., Kishi, H., Fukue, Y., Hirota, Y., Yoda, K., and Ohyama, T. (2003) Left-handedly curved DNA regulates accessibility to cis-DNA elements in chromatin, *Nucleic Acids Res.* **31**, 6651–6662.
15. Ohyama, T., Tsujibayashi, H., Tagashira, H., Inano, K., Ueda, T., Hirota, Y., and Hashimoto, K. (1998) Suppression of electrophoretic anomaly of bent DNA segments by the structural property that causes rapid migration, *Nucleic Acids Res.* **26**, 4811–4817.
16. Sambrook, J., Fritsch, E. F., and Maniatis, T. (1989) *Molecular Cloning: A Laboratory Manual*, 2nd ed., Cold Spring Harbor Laboratory Press, Plainview, NY.
17. Sasou, M., Sugiyama, S., Yoshino, T., and Ohtani, T. (2003) Molecular flat mica surface silanized with methyltrimethoxysilane for fixing and straightening DNA, *Langmuir* **19**, 9845–9849.
18. Matsugami, A., Tani, K., Ouhashi, K., Uesugi, S., Morita, M., Ohyama, T., and Katahira, M. (2006) Structural property of DNA which migrates fast in gel, as deduced by CD spectroscopy, *Nucleosides, Nucleotides, Nucleic Acids* **25**, 417–425.
19. Cowan, J. A. (1995) *The Biological Chemistry of Magnesium*, VCH Publishers, New York.
20. Ho, P. S., Frederick, C. A., Quingley, G. J., van der Marel, G. A., van Boom, J. H., Wang, A. H., and Rich, A. (1985) G·T wobble base-pairing in Z-DNA at 1.0 Å atomic resolution: The crystal structure of d(CGCGTG), *EMBO J.* **4**, 3617–3623.
21. Gessner, R. V., Quingley, G. J., van der Marel, G. A., van Boom, J. H., and Rich, A. (1985) Structural basis for stabilization of Z-DNA by cobalt hexaammine and magnesium cations, *Biochemistry* **24**, 237–240.
22. Travers, A. A. (2005) DNA dynamics: Bubble ‘n’ flip for DNA cyclisation? *Curr. Biol.* **15**, R377–R379.